

# Diblock Copolymer Ordering Induced by Patterned Surfaces Above the Order-Disorder Transition

Yoav Tsori and David Andelman\*

*School of Physics and Astronomy, Raymond and Beverly Sackler Faculty of Exact Sciences  
Tel Aviv University, 69978 Ramat Aviv, Israel  
(3/7/00)*

We investigate the morphology of diblock copolymers in the vicinity of flat, chemically patterned surfaces. Using a Ginzburg-Landau free energy, spatial variations of the order parameter are given in terms of a general two-dimensional surface pattern above the order-disorder transition. The propagation of several surface patterns into the bulk is investigated. The oscillation period and decay length of the surface  $q$ -modes are calculated in terms of system parameters. We observe lateral order parallel to the surface as a result of order perpendicular to the surface. Surfaces which has a finite size chemical pattern (e.g., a stripe of finite width) induces lamellar ordering extending into the bulk. Close to the surface pattern the lamellae are strongly perturbed adjusting to the pattern.

## I. INTRODUCTION

The bulk properties of diblock copolymers (BCP) are now well understood [1–5]. These long linear macromolecules composed of two incompatible sub-chains, or blocks, cannot phase separate because of the covalent bond between them. This connectivity, together with the incompatibility between the two blocks, gives rise to the appearance of microphase separated phases. The state of segregation is controlled by  $N\chi$  and  $f$ , where  $\chi$  is the Flory parameter,  $N = N_A + N_B$  is the total number of constituents monomers per chain and  $f$  is the fraction of the  $A$  block,  $f = N_A / (N_A + N_B)$ . For large enough  $N\chi$  one of the ordered phases, such as the lamellar, hexagonal or cubic phases is preferred, depending on the degree of asymmetry  $f$ .

Less understood is the interfacial behavior of copolymer melts near solid surfaces or at the free surface with air. Surface phenomena of BCP may enable creating and controlling technologically important devices of characteristic size comparable to the wavelength of light. As examples we mention waveguides, light-emitting diodes and other optoelectronic device, anti-reflection coating for optical surfaces [6] and dielectric mirrors [7].

The presence of a wall in a BCP system leads to new energy and length scales, depending on the specific chemical interaction of the polymers with the surface. In a semi-infinite system in contact with a single planar wall, the morphology near the surface can be very different from the bulk morphology. Fredrickson [8] has considered BCP in contact with a surface having a uniform preferential adsorption to one of the two blocks. Above the order-disorder transition (ODT), where  $\chi < \chi_c$  ( $\chi_c$  is the critical point value of  $\chi$  above which an ordered phase appears), he used mean-field theory and found that the order parameter (being the concentration differ-

ence between the two blocks) has decaying oscillations. He showed that the oscillation periodicity depends on  $\chi$ , and tends to the bulk lamellar periodicity as  $\chi \rightarrow \chi_c$ . In the same  $\chi \rightarrow \chi_c$  limit, the correlation length  $\xi$  of the oscillations was found to diverge. Further investigations [9] showed that the inclusion of higher order, non-linear corrections to the mean-field theory results in a non-diverging  $\xi$ . For the same system cooled below the ODT, modulated sinusoidal behavior was found. In a related work [10] a Ginzburg-Landau free energy was used to describe the propagation of a surface-induced lamellar ordering into a bulk hexagonal phase. In the strong-segregation limit a lamellar region of finite thickness close to the surface becomes stable, provided that the surface field is larger than some critical value.

The situation is even more complicated in thin films, where the distance between the two boundaries, associated with the film thickness, is comparable to the periodicity of modulations in the bulk, and the surface induced morphology can be of different symmetry than that of the bulk. For a system taken in one of its ordered phases (below the ODT), the free energy has a local minimum when the spacing between the surfaces is an integer multiple of the bulk repeat period. The mean-field behavior of BCP close to surfaces and for BCP films was calculated [11] using a method applicable in both the strong and weak segregation limits. It was found that confinement of lamellar phase BCP may lead to parallel layering, or in some cases even to a perpendicular arrangement of the lamellae. Self-consistent field theory (SCF) was used [12,13] to study the stability of these parallel, perpendicular and mixed lamellar phases in thin films of BCP. The latter phase consists of parallel lamellae near one surface and perpendicular lamellae near the opposite surface, but it was found to be unstable for symmetric A-B ( $f = 1/2$ ) diblock copolymers.

So far, we mentioned situations where the surfaces have

a uniform preference to one of the two blocks. More complex, chemically patterned surfaces break the lateral translation symmetry. Different surface regions will now have a different preference for the A/B blocks, thereby inducing a lateral structured morphology near the surface. Very few works took into account this possibility of a non-uniform surface. In particular, Petera and Muthukumar [14,15] have investigated the effect of a *one dimensional* sinusoidal surface pattern on BCP morphologies close to the surface in the weak-segregation limit, both below and above the ODT.

In this paper we consider a BCP melt above the ODT near a surface, whose pattern is truly arbitrary in two dimensions, generalizing the results of Refs. [14,15]. A Ginzburg-Landau free energy is expressed in term of the polymer concentration is presented in Sec. II. In Sec. III we consider a melt close to one surface or confined between two surfaces whose chemical pattern has one dimensional symmetry. Minimization of the free energy expansion gives rise to an Euler-Lagrange equation for the order parameter. A natural generalization to two-dimensional surface patterns is then considered in Sec. IV. We are able to give a complete description of the order parameter in terms of all the  $q$ -modes of the surface pattern. Finally, conclusions and some future prospects are presented in Sec. V.

## II. THE MODEL

The copolymer melt is described by the order parameter  $\phi(\mathbf{r})$ , defined as  $\phi(\mathbf{r}) = \phi_A(\mathbf{r}) - f$ , the difference in local A monomer concentration from its average value. Hereafter we restrict the treatment to the symmetric  $f = 1/2$  case, following the same coarse-grained free energy as was used by Fredrickson and Binder [16,17]:

$$\frac{N}{k_B T} F = \int \left\{ \frac{1}{2} \phi \left[ \tau + h (\nabla^2 + q_0^2)^2 \right] \phi + \frac{u}{4!} \phi^4 \right\} d^3 \mathbf{r} \quad (1)$$

Where  $k_B$  is the Boltzmann constant and  $T$  is the temperature. The other parameters are:

$$q_0 \approx 1.9456 / \sqrt{\langle R_g^2 \rangle} \quad (2)$$

$$\tau = 2\rho N (\chi_c - \chi) \quad (3)$$

$$\chi_c = 10.495/N \quad (4)$$

$$h = 1.5\rho c^2 \langle R_g^2 \rangle / q_0^2 \quad (5)$$

The fundamental wavelength of the system,  $q_0$ , is expressed by  $R_g$ , the radius of gyration of the chains. The chain density  $\rho$  is equal to  $1/Na^3$  for an incompressible melt, and  $u/\rho$  and  $c$  are of order unity. More details can be found in Ref. [17] and extensions for asymmetric BCP,  $f \neq 1/2$  are possible as well. The use of (1) limits our treatment to a region of the phase diagram close enough to the critical point where the expansion in powers of  $\phi$

and its derivatives is valid, but not too close to it, because then critical fluctuation effects may be important [18].

This and similar types of free energy has been used to describe bulk and surface phenomena in amphiphilic systems [20], diblock copolymers [3,4,17,19,21], Langmuir films [22] and magnetic (garnet) films [23]. The  $\phi^2$  and  $\phi^4$  terms appear in the usual Landau expansion. The added  $\phi \nabla^2 \phi$  and  $\phi \nabla^2 \nabla^2 \phi$  terms compete to produce *modulated phases* below the order-disorder temperature. This free energy describes a system in the disordered phase ( $\phi = 0$ ,  $f = 1/2$ ) for  $\chi < \chi_c$ , and in the lamellar phase for  $\chi > \chi_c$ . The  $q = q_0$  mode goes critical first, and the lamellar phase is described by  $\phi = \phi_q \cos(\mathbf{q}_0 \cdot \mathbf{r})$ , of repeat period  $d_0 \equiv 2\pi/q_0$ . This single-mode approximation is accurate to order  $(\chi - \chi_c)^{1/2}$  and can be justified near the critical point [8]. Far from the critical point higher harmonics are needed to describe the lamellar phase. As the asymmetry in composition is increased, other ordered phases of hexagonal and cubic symmetries become more stable than the lamellar phase.

As stated above, block copolymers exhibit complex surface behavior characterized by the strength and range of the interaction between the polymer chains and the surface, the typical size of chemical heterogeneities of the surface, and the distance between the two surfaces, in case of a thin film.

The presence of chemically interacting confining walls is modeled by an added short-range surface coupling term in the free energy,

$$F_s = \int d^2 \mathbf{r}_s (\sigma(\mathbf{r}_s) \phi(\mathbf{r}_s) + \tau_s \phi^2(\mathbf{r}_s)) \quad (6)$$

The vector  $\mathbf{r}_s$  define the position of the confining surfaces. The  $\sigma\phi$  term expresses the preferential interaction of the surface with the A and B blocks. For example, if  $\sigma > 0$  then the B block ( $\phi < 0$ ) is attracted to the surface more than the A block ( $\phi > 0$ ). Control over the specificity of this surface term can be achieved by coating the substrate with carefully prepared random copolymers [24,25]. The coefficient of the  $\phi^2$  term in (6),  $\tau_s$ , is a surface correction to the Flory parameter  $\chi$  [8,9,26].  $\tau_s > 0$  corresponds to a suppression of surface segregation of the A and B monomers.

We first consider systems in which the polymer melt is confined by a flat, rigid wall at  $y = 0$ , with the  $x$ -axis chosen in the plane of the wall, and is translational invariant along the  $z$ -direction. Extension to the system of two parallel surfaces located at  $y = \pm L$  is straightforward and will be considered later. The order parameter  $\phi$  is expected to vanish in regions where the interfacial interactions can be neglected,

$$\lim_{y \rightarrow \infty} \phi(x, y) = 0 \quad (7)$$

recovering the value  $\phi = 0$  of the bulk phase far from the surface. In the next section we find profile solutions

$\phi(x, y)$  for a BCP system at temperatures above the bulk ODT.

### III. ONE DIMENSIONAL SURFACE PATTERNS

For high enough temperatures, or equivalently, for  $\chi < \chi_c$ , the phase of lowest free energy is the homogeneous disordered phase, with  $\phi(\mathbf{r}) = 0$  in the bulk. The presence of a patterned surface induces ordering in the copolymer melt. If the chemical surface composition is uniform, one of the monomers, A or B, will be attracted to the surface, resulting in a parallel orientation of the lamellae (a perpendicular orientation of the chains). If the pattern is modulated, say sinusoidally, then different blocks are attracted to different regions of the surface. We will start with this case of a semi-infinite system bounded by one rigid, flat surface, and then proceed to describe thin film systems between two surfaces.

#### A. One patterned surface

Consider the semi-infinite BCP melt at  $y > 0$  bounded by a flat surface given by  $y = 0$ . We assume a one dimensional periodic surface pattern and write it in terms of the Fourier components of the surface field  $\sigma(x)$

$$\sigma(x) = \sum_q \sigma_q e^{iqx} \quad (8)$$

where  $\sigma_q$  set the amplitude of the respective  $q$ -modes. The order parameter  $\phi(x, y)$  satisfies the boundary conditions on the surface and approaches the bulk solution far from the surface. It is convenient to decompose  $\phi$  in terms of its  $q$ -modes in the  $x$ -direction

$$\phi(x, y) = \sum_q f_q(y) e^{iqx} \quad (9)$$

The requirement (7) leads to the bulk boundary condition

$$\lim_{y \rightarrow \infty} f_q(y) = 0 \quad (10)$$

The form (9) is substituted in (1). Above the order-disorder transition (ODT) temperature, the theory is stable to second order in  $\phi$ , and therefore the  $\phi^4$  term is neglected. Using the explicit  $x$ -dependence of  $\phi$  in (9) we perform the  $x$  and  $z$  integration, yielding the free energy  $F$ :

$$\begin{aligned} F = & \int \sum_q \left\{ (\tau + h q_0^4) f_q f_q^* + h q_0^2 \left[ f_q (f_q'' - q^2 f_q)^* + c.c. \right] \right. \\ & + \frac{1}{2} h \left[ f_q (f_q'''' - 2q^2 f_q'' + q^4 f_q)^* + c.c. \right] \Big\} dy \\ & + \sum_q (\sigma_q f_q^*(0) + \tau_s f_q(0) f_q^*(0)) + c.c. \end{aligned} \quad (11)$$

where (...) indicates complex conjugation (c.c.) operation. A standard minimization technique is carried on and yields the governing linear ordinary differential equation for the functions  $\{f_q\}$  for  $y > 0$ :

$$\left( \tau/h + (q^2 - q_0^2)^2 \right) f_q + 2(q_0^2 - q^2) f_q'' + f_q'''' = 0 \quad (12)$$

This equation possesses four independent solutions in the form of an exponential  $e^{-k_q y}$ , with  $k_q$  found from the characteristic equation

$$\left( \tau/h + (q^2 - q_0^2)^2 \right) + 2(q_0^2 - q^2) k_q^2 + k_q^4 = 0 \quad (13)$$

Thus, with the semi-infinite geometry, the solution is

$$f_q(y) = A_q e^{-k_q y} + B_q e^{-k_q^* y} \quad (14)$$

and

$$k_q^2 = q^2 - q_0^2 + i(\tau/h)^{1/2} \quad (15)$$

Each  $q$ -mode solution  $f_q$  is characterized by two complex amplitudes  $\{A_q, B_q\}$ . From the solutions of Eq. (13) wavevectors  $\{k_q\}$  with negative real value,  $\text{Re}(k_q) < 0$ , are discarded, to comply with the boundary condition (10). Note that  $\text{Re}(k_q)$  is increasing monotonously as a function of  $q$ . A large value of  $\text{Re}(k_q)$  means short decay length, and hence the smallest surface  $q$ -mode decays the least. This behavior is demonstrated on Fig. 1 showing the  $q$  and  $\chi$  dependence of the real and imaginary parts of the wave-vector  $k_q$ . For a fixed value of  $\chi$  the decay length, proportional to  $1/\text{Re}(k_q)$ , decreases as  $q$  increases, while the wavelength  $2\pi/\text{Im}(k_q)$  of the modulations in  $f_q(y) \sim e^{-k_q y}$  increases.

The boundary conditions for the functions  $f_q$  can be determined by considering the Euler-Lagrange equation for  $\{f_q\}$  in the range that includes  $y = 0$ . In this case a term proportional to the Dirac delta function  $\delta(y)$  appears in (12). There are two conditions relating  $f_q$  and its derivatives at  $y = 0$ :

$$f_q''(0) + 2(q_0^2 - q^2) f_q(0) = 0 \quad (16)$$

$$\frac{2\sigma_q}{h} + \frac{4\tau_s}{h} f_q(0) + 2(q_0^2 - q^2) f_q'(0) + f_q''(0) = 0 \quad (17)$$

Recently, it has been found [28] that surface states exist even in the absence of a surface field  $\sigma$ . This effect can be attributed to a loss of entropy close to the surfaces. However, in our linear theory this does not happen, and the copolymer response is proportional to the surface field  $\sigma$ . The case where  $\sigma_0$  is a non-zero constant and  $\sigma_{q \neq 0} = 0$ , corresponds to the special case of uniform interfacial interactions. The system exhibits a decaying lamellar layering of the polymers, with the B-polymer adsorbed to the surface if  $\sigma_0 > 0$ .

Close to the ODT, the complex wavevector  $k_0$  can be approximated by

$$k_0 \simeq -\frac{(\tau/h)^{1/2}}{2q_0} + iq_0 \left(1 - \frac{\tau/h}{8q_0^4}\right) \quad (18)$$

This expression shows that  $f_0 \sim e^{-k_0 y} \sim e^{-y/\xi}$  has a diverging characteristic length  $\xi \propto (\chi_c - \chi)^{-1/2}$ , while the oscillatory part has a wavelength slightly longer than that of the bulk lamellar phase, in agreement with the results of Fredrickson for chemically uniform surfaces [8]. The correlation length  $\xi$  diverges for small composition oscillations because a linear theory is employed; addition of the  $\phi^4$  term in  $F$  would give a finite value of  $\xi$ . As a result of the assumed short-range surface interactions, the periodicity and decay length of  $f_q$  depend only on properties of the bulk, and not on surface details.

Using the notation  $k_q = k'_q + ik''_q$  the real part of the form (14) can be rewritten as:

$$\begin{aligned} 2\text{Re}(f_q) &= (A_q + B_q^*) e^{-k_q y} + c.c. \\ &= 2|A_q + B_q| e^{-k'_q y} \cos(k''_q y + \alpha_q) \end{aligned} \quad (19)$$

where  $\alpha_q$  is the phase of the  $q$ -mode modulation. It determines the value of the  $f_q$  solution at the boundary,  $y = 0$ .

The phase  $\alpha_0$  for the  $q = 0$  mode is found to satisfy the following relation

$$\tan \alpha_0 = \frac{q_0^2}{\sqrt{\tau/h}} \quad (20)$$

and therefore is determined by the degree of segregation  $\chi$ , but not by the pattern amplitude  $\sigma_q$ . A plot of  $\alpha_q$  as a function of  $q$  for several values of  $\chi$  is shown in Fig. 2 (a). Far from the ODT point and deep into the disordered phase,  $\chi \ll \chi_c$ , we find that all  $q$ -modes have a phase angle  $\alpha_q = 0$ . As the ODT is approached, the  $q = q_0$  mode retains its value but larger  $q$ -modes have a negative phase while smaller  $q$ -modes have a positive phase. At  $\chi = \chi_c$  this becomes a step function, with  $\alpha_q = \pi/2$  for  $q < q_0$  and  $\alpha_q = -\pi/2$  for  $q > q_0$ . The amplitude behavior is shown in Fig. 2 (b), for the same series of segregation values  $\chi$ . As the ODT is approached, the  $q = q_0$  mode becomes critical first, with a diverging amplitude.

An interesting limit occurs when  $\sigma_0 = 0$ , that is, the average surface interaction is zero (no net adsorption). No lamellar ordering parallel to the surface is expected. Indeed, the resulting checkerboard behavior is illustrated for a surface pattern chosen for simplicity to contain only one mode:  $\sigma(x) = \sigma_q \cos(qx)$ . Fig. 3 depicts alternating A-rich (white) and B-rich (black) regions. In (a) the decay length  $\xi$  is smaller than in (b), because in the former case the surface periodicity is twice as large. The oscillatory behavior, characterized by  $\text{Im}(k_q)$ , has a very long wavelength, diverging as  $(\chi_c - \chi)^{-1/2}$  close to the ODT point.

Usually, if no special measures are taken [24,25], there is a net preference to one of the monomers:  $\sigma_0 \neq 0$ .

The BCP morphology where the surface interactions were chosen to have both a non-zero average preference and undulatory character, namely  $\sigma = \sigma_0 + \sigma_q \cos(qx)$ , is shown in Fig. 4. A smooth crossover from surface-induced ordering at small distance to the bulk disorder occurs. The parallel lamellae resulting from the  $\sigma_0$  term persist farther from the surface than the bulges resulting from the  $\sigma_q$  term, as  $f_0$  decays slower than  $f_q$ . For a given  $\sigma_0$ , having a higher  $q$ -mode or reducing the modulation strength  $\sigma_q$  will enhance the lamellar features far from the surface.

## B. Two patterned surfaces

Until now the BCP melt was assumed to be bounded by one surface at  $y = 0$ . In this section we extend our analysis to a thin-film system confined between two parallel surfaces located at  $y = L$  and  $y = -L$ , shown in Fig. 5. When the distance  $2L$  between the surfaces is comparable to the natural bulk periodicity, the two surfaces interact via the BCP and the resulting film morphology can be very different from that of the one-surface case (Sec. III A). However, the mathematical analysis is almost the same; one only has to apply different boundary conditions on the BCP order parameter  $\phi$ .

The surfaces at  $y = \pm L$  are assumed to carry different surface fields of the form  $\sigma^\pm(x) = \sum_q \sigma_q^\pm e^{iqx}$ . Only small modifications must be included to adjust the results of the previous section. The same ansatz (9) for  $\delta\phi$  is used. The functions  $f_q$  that minimize the appropriate  $x$ -averaged free energy (1) obey

$$f_q(y) = A_q e^{-k_q y} + B_q e^{-k_q^* y} + C_q e^{k_q y} + D_q e^{k_q^* y} \quad (21)$$

with  $\{k_q\}$  given by the same relation (15). However, unlike the semi-infinite bulk one-surface case (14), both signs of the  $k$  vectors are used because the system is finite in the  $y$ -direction. In addition, repeating the procedure outlined for the one-surface case, gives the boundary conditions for  $f_q$ :

$$f_q''(\pm L) + 2(q_0^2 - q^2) f_q(\pm L) = 0 \quad (22)$$

$$\begin{aligned} \frac{2\sigma_q^\pm}{h} + \frac{4\tau_s}{h} f_q(\pm L) \\ \mp 2(q_0^2 - q^2) f_q'(\pm L) \mp f_q'''(\pm L) = 0 \end{aligned} \quad (23)$$

We consider now several specific surfaces. In the first  $\sigma^+ = 1$  is a constant, while  $\sigma^- = \cos(qx)$  is purely sinusoidal and average to zero, as depicted in Fig. 6. As expected, the B polymer (in black) is attracted to the upper surface, while the bottom surface exhibits modulated adsorption pattern. Although lamellar features are seen near the top surface, the overall apparent phase in the sample cannot be classified as such. The corresponding plots of the functions  $f_0(x)$  and  $f_q(x)$  are shown in Fig. 7 (same parameters as in Fig. 6). In general  $f_q$  is nonzero even at the  $y = L$  surface, although the surface

does not induce modulations by itself,  $\sigma^+ = \text{const}$ . Thus modulations propagate from one surface to the other by the copolymer melt. This is an interesting observation which may have relevance in applications. It relies on the relative small thickness of the BCP film.

The situation as depicted in Fig. 6 represents a competition between two mechanisms. The modulated pattern at the bottom surface induces a laterally modulated pattern of the BCP, while the top surface uniform interaction induces a lamellar-like layering of the copolymers. As the modulated adsorption pattern strongly depends on the modulation wavenumber, so does the resulting morphology. This effect is shown explicitly in Fig. 8, where the top surface is uniform and the bottom is modulated, for a series of  $q/q_0$  values. The transition from a locally perpendicular (bottom patterned surface) to a locally parallel orientation (at the top uniform surface) is seen in (a), similar to the so-called T-junctions between grains of different orientations [21,29]. Similar behavior was found by the SCF calculation in Ref. [15].

Figure. 9 (a) shows the spatial dependence of the BCP order parameter when the two surfaces contain only one  $q$ -mode and are patterned *in phase* with each other (symmetric arrangement), but with opposite signs,  $\sigma^\pm = \pm \sigma_q \cos(qx)$ . The copolymer patterns create a perfect checkerboard arrangement and are related to each other at the surfaces by an interchange of monomers  $A \leftrightarrow B$ . The surface pattern (8) contains only  $\cos(qx)$  terms. A generalization that includes  $\sin(qx)$  sinusoidally varying modes is straightforward. In this case the patterns at the surfaces can be out-of-phase with each other. Figure. 9 (b) shows such a morphology, for  $\sigma^+ = \sigma_q \cos(qx)$ ,  $\sigma^- = \sigma_q \sin(qx)$ , where there is a  $\pi/2$  phase shift between the two surface fields. The perfect checkerboard arrangement of 9 (a) is now distorted to accommodate this phase shift.

#### IV. TWO-DIMENSIONAL SURFACE PATTERNS

So far we considered a melt in contact with a surface or confined between two surfaces of one dimensional symmetry. In our approximation, like in any linear response theory, there is no  $q$ -mode coupling proportional to  $\sigma_{q_1} \sigma_{q_2}$ . This fact allows us to go further and introduce a two-dimensional generalization of the surface pattern, which so far was taken to be independent on  $z$ . The surface now is assumed to carry a chemical pattern  $\sigma(x, z)$  which can be written as:

$$\sigma(x, z) = \sum_{q_x, q_z} \sigma_{q_x, q_z} e^{i(q_x x + q_z z)} \quad (24)$$

The “linear response” function is then

$$\delta\phi(x, y, z) = \sum_{q_x, q_z} f_{q_x, q_z}(y) e^{i(q_x x + q_z z)} \quad (25)$$

Because  $f$  and  $\sigma$  are real functions,  $f_{-q_x, -q_z} = f_{q_x, q_z}^*$  and similarly for  $\sigma$ . Using the above form it is possible to carry out the integration of the free energy in the  $x-z$  plane. Denoting  $\langle \dots \rangle_{xz}$  as the average in the  $x-z$  plane, it can be checked, for example, that

$$\langle \phi \nabla^2 \phi \rangle_{xz} = \sum_{q_x, q_z} f_{q_x, q_z} (f_{q_x, q_z}'' - (q_x^2 + q_z^2) f_{q_x, q_z})^* \quad (26)$$

Defining  $\mathbf{q}_\parallel \equiv (q_x, q_z)$  and performing the free energy minimization with respect to  $f_{q_x, q_z}^*$ , the functions  $f_{q_\parallel} = f_{q_x, q_z}$  obey the same master equation (12) that  $f_q$  previously obeyed, with the only change that  $q^2$  is replaced by  $q_\parallel^2$ . For a BCP in contact with a single surface, the appropriate boundary conditions are:

$$\begin{aligned} f_{q_\parallel}''(0) + 2(q_0^2 - q_\parallel^2) f_{q_\parallel}(0) &= 0 \\ \frac{2\sigma_{q_\parallel}}{h} + \frac{4\tau_s}{h} f_{q_\parallel}(0) + 2(q_0^2 - q_\parallel^2) f_{q_\parallel}'(0) + f_{q_\parallel}'''(0) &= 0 \end{aligned} \quad (27)$$

The solution for  $f_{q_\parallel}$  is analogous to (14),

$$f_{q_\parallel}(y) = A_{q_\parallel} e^{-k_{q_\parallel} y} + B_{q_\parallel} e^{-k_{q_\parallel}^* y} \quad (28)$$

$$k_{q_\parallel}^2 = q_\parallel^2 - \frac{1}{2} + i(\chi_c - \chi)^{1/2} \quad (29)$$

Having found the response of the polymers to the surface modes  $\sigma_{q_\parallel}$ , one is able to deduce the concentration profiles for any given two-dimensional surface pattern. In order to illustrate this, we take a system of chemical affinity in the shape of the letters “BCP” on the  $y = 0$  surface [Fig. 10 (a)], and calculate the polymer concentration in the planes parallel and above it. All sizes are expressed in terms of  $d_0$ , the lamellar fundamental periodicity. The shape of the letters continuously deforms as one moves away from the surface. Contour plots corresponding to planes parallel to the  $x-z$  surface and separated by a distance  $(n + 1/2)d_0$ , for integer  $n$ , are approximately given by an  $A \leftrightarrow B$  interchange of monomers. This is the characteristic distance at which the polymers flip. Note that Fig. 10 (c) and (e) are approximately the inverse image (“negative”) of (b), (d) and (f). The original features are completely washed away as the distance  $y$  from the surface is further increased. In our case for  $5d_0 \lesssim y \lesssim 6d_0$  where the surface pattern size was roughly  $d_0$ .

Figure 10 also illustrates circumstances where a certain surface pattern is transferred via the bulk BCP to another, distant surface. It may be important to know, for example, if the contrast of the distant image can be experimentally detected. This reduction of the contrast is clearly seen by comparing Fig. 10 (b) and (f), and can easily be calculated from our expressions. The lamellar order created parallel to the edges of the letters in Fig. 10 (b) is the result of the undulatory nature of the block copolymers: order extending perpendicular to the surface induces order in the direction parallel to it.

The copolymer melt can follow the surface pattern when its size is larger than the polymer length-scale  $d_0$ . The effect of reducing the size of the surface structure is seen as a blurred morphology in Fig. 11 (a), where the “BCP” pattern was chosen to have dimensions  $4d_0 \times 4d_0$ , compare to  $20d_0 \times 20d_0$  of Fig. 10 (b). The effect of raising the temperature (further away from the ODT) is seen in Fig. 11 (b). It is similar to Fig. 10 (b), only that the temperature is higher,  $N\chi = 9$ , and the lamellar features along the edges of the letter are less prominent. Again, using our order parameter expressions one can quantify the  $q$ -mode spectrum and contrast of the distant image, as a function of the original surface pattern  $\sigma(x, z)$ , temperature and distance from the  $y = 0$  surface.

In a thin film, creation of truly three dimensional, complex morphologies between the two surfaces can be achieved by using only one-dimensional surface patterns. As an example we choose a simple sinusoidal pattern on each of the  $y = \pm L$  surfaces, rotated 90 degrees with respect to one another:  $\sigma^- = \cos(qx + qz)$  and  $\sigma^+ = \cos(qx - qz)$ . In Fig. 12(b) the resulting morphology in the  $y = 0$  mid-plane is shown and is a superposition of the two surface patterns. Because  $y = 0$  is a symmetric plane, the pattern has a square symmetry. More complex patterns can be created at different  $y$  planes.

In Sec. III we showed that the  $q = 0$  mode of the surface pattern is the slowest decaying mode, resulting in a lamellar layering parallel to the surface as  $y \rightarrow \infty$ , no matter what the surface pattern is. We demonstrate this in Fig. 13, where in (a) we choose a simple one-dimensional structure in the shape of a stripe of width  $d_0$ . Inside the stripe of width  $d_0$ ,  $\sigma(x, z) = 0.5$  while outside it, the surface area is neutral,  $\sigma = 0$ . Thus, the B-polymer is preferentially adsorbed onto the stripe. The order parameter contour plot in the  $x - y$  plane is shown in (b). It can be seen that the “surface disturbance” is enclosed with alternating lamellae. The distorted lamellae close to the  $y = 0$  surface appear curved, and slowly fade away as the distance from the surface is increased.

A different scenario is presented in Fig. 14, where inside the stripe of thickness  $d_0$ ,  $\sigma = 0.5$  as above, but outside the stripe the surface is not neutral:  $\sigma = -0.5$ . We find that the adsorption on the surface is quite different than in Fig. 13. Far from the stripe, the A-polymer is adsorbed onto the surface and induces stacking of the BCP in a direction parallel to the surface. Close to the surface perturbation (the stripe) the behavior is altered as the lamellae are strongly deformed in order to optimize their local interaction with the surface stripe.

## V. CONCLUSIONS

We have employed a simple Ginzburg-Landau expansion of the BCP free energy to study analytically the confinement effects of block copolymers between two patterned surfaces as well as the interfacial behavior of a

BCP close to a patterned surface. Our approach consists of finding the governing equation for a presumably small perturbation to the bulk order parameter, by retaining second-order terms in the free energy. This approach can be justified in the vicinity of the critical point. Above the ODT it gives rise to a simple linear equation with fixed coefficients [8,14]. A generalization to two-dimensional surface patterns is presented, where a complete spatial description of the polymer concentration is given in terms of an arbitrary surface pattern. However, this approach applies to systems below the ODT as well, where a linearization is to be taken around an ordered phase [30,31].

The assumption that the surface interactions are strictly local means that the length scales of the polymer morphology are determined by bulk properties. Moreover, each of the surface  $q$ -modes in  $\sigma(x) = \sum_q \sigma_q \cos qx$  gives rise to a corresponding mode  $f_q \cos qx$  in the local polymer concentration  $\phi(x, y)$ . This “response” mode is characterized by a single wavevector  $k_q$ . The wavevector  $k_q$  is determined by  $\chi$  and the surface wavenumber  $q$ . In Fig. 1 we show the dependence of  $k_q$  on these parameters. The high  $q$ -modes of the surface pattern  $\sigma(x, z)$  decay more rapidly than those of low  $q$ . For high  $q$ -modes of characteristic length scale much smaller than the polymer chains  $d_0$ , the BCP melt cannot follow the surface modulations, and feels just the average of those modulations (which is zero for  $q > 0$ ). This dependence of  $k_q$  on  $q$  and  $\chi$  is very similar to the results found by Petera and Muthukumar [14] using a different free-energy functional.

Moreover, we generalized surface patterns to any two-dimensional patterns as can be seen in Fig. 10. Even within a mode decoupled (linear response) theory, many interesting effects follow for a single surface as well as for films confined between two surfaces. Tuning a few surface parameters can lead to controlled micro-structures of the BCP film.

For a BCP melt in contact with a homogeneous surface, a decaying lamellar order appears. The phase  $\alpha_0$  of these sinusoidally damped oscillations obeys  $\tan \alpha_0 = q_0^2 / \sqrt{\tau/h}$ , and it is independent of the surface pattern amplitude  $\sigma_0$  [17]. For high temperatures all  $q$ -modes have the same phase  $\alpha_q = 0$ . As  $\chi \rightarrow \chi_c$ , the  $q = q_0$  retains this value, while higher  $q$ -modes tend to  $-\pi/2$ , and lower  $q$  tend to  $\pi/2$ . At the same limit the  $q = q_0$  mode gets critical first, with a diverging amplitude.

Our expressions for the spatial dependence of the order parameter on a general patterned surface gives a complete description of the system, and allows for the calculation of free energy, pressure, etc. It may also help in tuning the required distance between the two surfaces in various applications. Using a strong enough surface field or fixing the conditions close to the ODT, one can hope to transform a pattern from one surface to the other surface. We also demonstrate in Fig. 12 how the superposition of simple one dimensional patterns can bring about a three dimensional behavior in a thin film system. A desired complex phase can then be achieved by tuning the Flory parameter and the relevant distances.

Possible extension to this work will be to calculate the phase diagram of the  $L_{\perp}$  phase (a confined lamellar phase where lamellae are perpendicular to the confining surfaces) vs. the  $L_{\parallel}$  phase (where the lamellae are parallel to the surfaces), by calculating the surface contribution to the bulk free energy in  $F$  (1). In the weak segregation limit this contribution is important and may lead to a completely different diagram than that of the strong segregation regime.

## ACKNOWLEDGMENTS

We would like to thank S. Herminghaus, G. Krausch, M. Muthukumar, R. Netz, G. Reiter, T. Russell, M. Schick and U. Steiner for useful discussions. Partial support from the U.S.-Israel Binational Foundation (B.S.F.) under grant No. 98-00429 and the Israel Science Foundation founded by the Israel Academy of Sciences and Humanities — centers of Excellence Program is gratefully acknowledged.

- 
- [1] Bates F. S.; Fredrickson G. H. *Annu. Rev. Phys. Chem.* **1990**, *41*, 525.
  - [2] Ohta K.; Kawasaki K. *Macromolecules* **1986**, *19*, 2621.
  - [3] Leibler, L. *Macromolecules* **1980**, *13*, 1602.
  - [4] Fredrickson G. H.; Helfand E. *J. Chem. Phys.* **1987**, *87*, 697.
  - [5] Matsen M. W.; Bates F. *Macromolecules* **1996**, *29*, 7641.
  - [6] Walheim S.; Schäffer E.; Mlynek J.; Steiner U. *Science* **1999**, *283*, 520.
  - [7] Fink Y.; Winn J. N.; Fan S.; Chen C.; Michel J.; Joannopoulos J. D.; Thomas E. L. *Science* **1998**, *282*, 1679.
  - [8] Fredrickson G. H. *Macromolecules* **1987**, *20*, 2535.
  - [9] Tang H.; Freed K. F. *J. Chem. Phys.* **1992**, *97*, 4496.
  - [10] Turner M. S.; Rubinstein M. R.; Marques C. M. *Macromolecules* **1994**, *27*, 4986.
  - [11] Shull K. R. *Macromolecules* **1992**, *25*, 2122.
  - [12] Matsen M. W. *J. Chem. Phys.* **1997**, *106*, 7781.
  - [13] Geisinger T.; Mueller M.; Binder K. *J. Chem. Phys.* **2000**, *111*, 5241.
  - [14] Petera D.; Muthukumar M. *J. Chem. Phys.* **1997**, *107*, 9640.
  - [15] Petera D.; Muthukumar M. *J. Chem. Phys.* **1998**, *109*, 5101.
  - [16] Fredrickson, G.H.; Binder K. *J. Chem. Phys.* **1989**, *91*, 7265.
  - [17] Binder K.; Frisch H. L.; Stepanow S. *J. Phys. II* **1997**, *7*, 1353.
  - [18] Brazovskii S. A., *Sov. Phys. JETP* **1975**, *41*, 85.
  - [19] Tsori Y; Andelman D.; Schick M. *Phys. Rev. E.* **2000**, *61*, 2848.
  - [20] Gompper G.; Schick M. *Phys. Rev. Lett.* **1990**, *65*, 1116.
  - [21] Netz R. R.; Andelman D.; Schick M. *Phys. Rev. Lett.* **1997**, *79*, 1058.
  - [22] Andelman D.; Brochard F.; Joanny J.-F. *J. Chem. Phys.* **1987**, *86*, 3673.
  - [23] Garel T.; Doniach S. *Phys. Rev. B* **1982**, *26*, 325.
  - [24] Kellogg G. J.; Walton D. G.; Mayes A. M.; Lambooy P.; Russell T. P.; Gallagher P. D.; Satija S. K. *Phys. Rev. Lett.* **1996**, *76*, 2503.
  - [25] Mansky P.; Russell T. P.; Hawker C. J.; Mayes J.; Cook D. C.; Satija S. K. *Phys. Rev. Lett.* **1997**, *79*, 237.
  - [26] Kielhorn L.; Muthukumar M. *J. Chem. Phys.* **1997**, *111*, 2259.
  - [27] Villain-Guillot S.; Netz R. R.; Andelman D.; Schick M. *Physica A* **1998**, *249*, 285. Villain-Guillot S.; Andelman D. *Euro. Phys. J. B* **1998**, *4*, 95.
  - [28] Jacobs A. E.; Mukamel D.; Allender D. W. *Phys. Rev. E* **2000**, *61* 2753.
  - [29] Gido S. P.; Thomas E. L. *Macromolecules* **1994**, *27*, 6137.
  - [30] Tsori Y.; Andelman D. submitted to *EuroPhys. Lett.*
  - [31] Tsori Y.; Andelman D. to be published.

• **Fig. 1:** The real (a) and imaginary (b) parts of the wavevector  $k_q$  as a function of the modulation  $q$ -mode and the Flory parameter  $N\chi$ . For values of  $N\chi$  close to its critical value,  $N\chi_c = 10.495$ , and for small  $q$ ,  $\text{Re}(k_q)$  is small. As  $q$  increases  $\text{Re}(k_q)$  starts to increase rapidly and  $\text{Im}(k_q)$  decreases. The value and magnitude of this sharp change in  $k_q$  are determined by the proximity to ODT. Farther from the critical point (smaller  $\chi < \chi_c$ ) the variation of  $k_q$  with  $q$  are smoothed out.

• **Fig. 2:** (a) A plot of the phase angle  $\alpha_q$  from Eq. (19), as a function of the surface  $q$ -mode, for different Flory parameters  $N\chi$ . Circles, dotted, diamond and dashed lines correspond to  $N\chi = 6.9, 8.5, 9.3$  and  $10.2$ , respectively. The solid line is for  $N\chi = N\chi_c$ . Far from the ODT point (high temperatures,  $\chi \ll \chi_c$ ), all  $q$ -modes have phases equal to zero, creating a quarter-lamella region of adsorption near the surface. In the opposite limit, i.e. when  $\chi \lesssim \chi_c$ ,  $q$ -modes with  $q < q_0$  have  $\alpha_q \rightarrow \pi/2$ , while the  $q$ -modes with  $q > q_0$  have  $\alpha_q \rightarrow -\pi/2$ .

In (b) are shown the surface amplitudes  $|A_q + B_q^*|$  from Eq. (19), as a function of the  $q$ -mode, for the same series of  $\chi$  values as in (a). As  $\chi \rightarrow \chi_c$ , the  $q = q_0$  mode goes critical first, with a diverging amplitude.

• **Fig. 3:** A contour plot of the BCP order parameter  $\phi(x, y)$ , where the surface pattern (bottom line,  $y = 0$ ) contains only one mode:  $\sigma(x) = \sigma_q \cos(qx)$ , with  $\sigma_q = 1$ . A-rich regions are black while B-rich are white. In (a),  $q = q_0$  while in (b)  $q = 0.5q_0$ . The decay length  $\xi$  is smaller in (a) than in (b) because the surface  $q$  mode is larger. The Flory parameter was set to  $N\chi = 10.4 < N\chi_c$ .

• **Fig. 4:** A contour plot of the BCP order parameter close to the critical point ( $N\chi = 10.4$ ). The surface pattern at  $y = 0$  is  $\sigma(x) = \sigma_0 + \sigma_q \cos(qx)$ , where  $\sigma_0$  is the average preference and  $q = \frac{2}{3}q_0$  is the modulation  $q$ -mode, with amplitudes  $\sigma_0 = \sigma_q = 0.1$ . The  $q = 0$  surface mode has a longer range effect than the  $q > 0$  surface mode, and induces parallel lamellar arrangement farther away from the surface. At yet larger distances the order parameter decays to its bulk  $\phi = 0$  value.

• **Fig. 5:** A sketch of a thin-film system confined between two surfaces. The  $y$  axis is perpendicular to the two parallel surfaces, located at  $y = \pm L$ . The  $z$  axis is out of the plane of the paper.

• **Fig. 6:** Polymer order parameter for a system of homogeneous interactions  $\sigma^+ = 1$  at  $y = L = 1.5d_0$  surface and modulated interactions at the opposite surface  $\sigma^- = \cos(qx)$ ,  $y = -L$ . The surface modulation wavenumber was chosen to be  $q = 0.5q_0$ . As

expected, the B polymer (shown in black) is preferentially attracted to the upper surface, while the bottom surface exhibits modulated adsorption pattern. This pattern propagates to the top surface. The Flory parameter was chosen  $N\chi = 10.4$ .

• **Fig. 7:** The two amplitude functions  $f_0(y)$  (dashed line) and  $f_q(y)$  (solid line) from Fig. 6 plotted against  $y/d_0$ .  $f_0$  is negative at  $y = L$  (top uniform surface of Fig. 6), and  $f_q$  is negative at the opposite modulated surface,  $y = -L$ . Notice that the pattern at  $y = -L$  induces order at the vicinity of the other surface, as  $f_q(L) \neq 0$ , although  $\sigma^+ = \text{const}$ .

• **Fig. 8:** A system of modulated surface  $\sigma^- = \cos(qx)$  at  $y = -L = -1.5d_0$  and of uniform  $\sigma^+ = 1$  at the opposite surface,  $y = L = 1.5d_0$ , for a series of different values of  $q/q_0$ . The effect of changing the repeat period  $q$  is clearly seen when  $q/q_0$  varies: 1 in (a), 2/3 in (b), 1/3 in (c). In all cases,  $N\chi = 10.2$ .

• **Fig. 9:** The crystalline-like checkerboard character of polymer order parameter. In (a) two patterned surfaces in phase with one another, but opposite in sign:  $\sigma^+ = -\sigma^- = \sigma_q \cos(\frac{1}{2}q_0x)$ . In (b) the patterns are  $\pi/4$  out of phase:  $\sigma^+ = \sigma_q \cos(\frac{1}{2}q_0x)$ ,  $\sigma^- = \sigma_q \sin(\frac{1}{2}q_0x)$ . The amplitude is  $\sigma_q = 0.2$ ,  $N\chi = 10.4$ , and the top and bottom surfaces are located at  $y = \pm 1.25d_0$ .

• **Fig. 10:** Propagation of surface order into the bulk. (a) is the original chemical pattern (the letters “BCP”) at the  $y = 0$  surface, whose size is  $20 \times 20$  in units of  $d_0$ . White corresponds to A-block preferring regions. A sequence of contour plots for  $y = 0.5, 2d_0, 3.5d_0, 5d_0$  and  $6.5d_0$  are shown in (b), (c), (d), (e) and (f), respectively. The original pattern is gradually fading (small features, high  $q$ -modes first) as  $y$  is increased, until it is completely washed out. For  $y \approx (n + \frac{1}{2})d_0$  with  $n$  integer, there is an inversion of the original pattern, as the A (white) and B block (black) are interchanged relatively to the original pattern. The Flory parameter is taken as  $N\chi = 9.5$ .

• **Fig. 11:** Contour plots as in Fig. 10, but in (a) the surface pattern is reduced to smaller size of about  $4d_0 \times 4d_0$ , while in (b) size is as in Fig. 10 but the temperature is higher,  $N\chi = 9$ . The lamellar features along the letter are less prominent than in Fig. 10 (b). Note that in (b) the bulk ordering cannot tightly follow the surface pattern when the pattern size becomes comparable to  $1d_0$ , as in (a).

• **Fig. 12:** Creation of a complex three dimensional morphology by superposition of two one-dimensional surface patterns:  $\sigma^- = \cos(qx + qz)$  and  $\sigma^+ = \cos(qx - qz)$ . Shown is the thin film BCP



morphology, where (a) is the surface pattern at the  $y = -L = -d_0$  surface and (c) is the pattern at  $y = L = d_0$ . A contour plot of the order parameter in the mid-plane,  $y = 0$ , is shown in (b), depicting A-rich and B-rich regions with square symmetry. The Flory parameter is taken as  $N\chi = 9$  and  $q = q_0/3$ .

- **Fig. 13:** Appearance of curved lamellae as a result of a one-dimensional surface pattern along the  $z$  surface axis. In (a) is surface stripe is shown in the  $x - z$  plane. The (white) stripe has a surface field of  $\sigma = 0.5$  inducing preferential adsorption of the B-polymer. The rest of the surface (denoted by a grey color outside the stripe) has  $\sigma = 0$  and is indifferent to A/B adsorption. (b) is a contour

plot in the  $x - y$  plane, depicting curved lamellae surrounding the “disturbance” at the middle. As the distance from the stripe is increased more than  $10d_0$  shown here, the lamellae gradually fade away. The Flory parameter is taken to be  $N\chi = 10$ .

- **Fig. 14:** Same as in Fig. 13, but with  $\sigma = 0.5$  inside the stripe (white), while the rest of the surface (black) has  $\sigma = -0.5$ . In (a) the  $x - z$  surface is shown while in (b) the contour plots are shown in the  $x - y$  plane. Far from the stripe the B-polymer (in black) is adsorbed to the surface, and overall a lamellar morphology parallel to the surface is seen. Close to the stripe disturbance these lamellae are modified, distorted locally by the presence of the stripe.

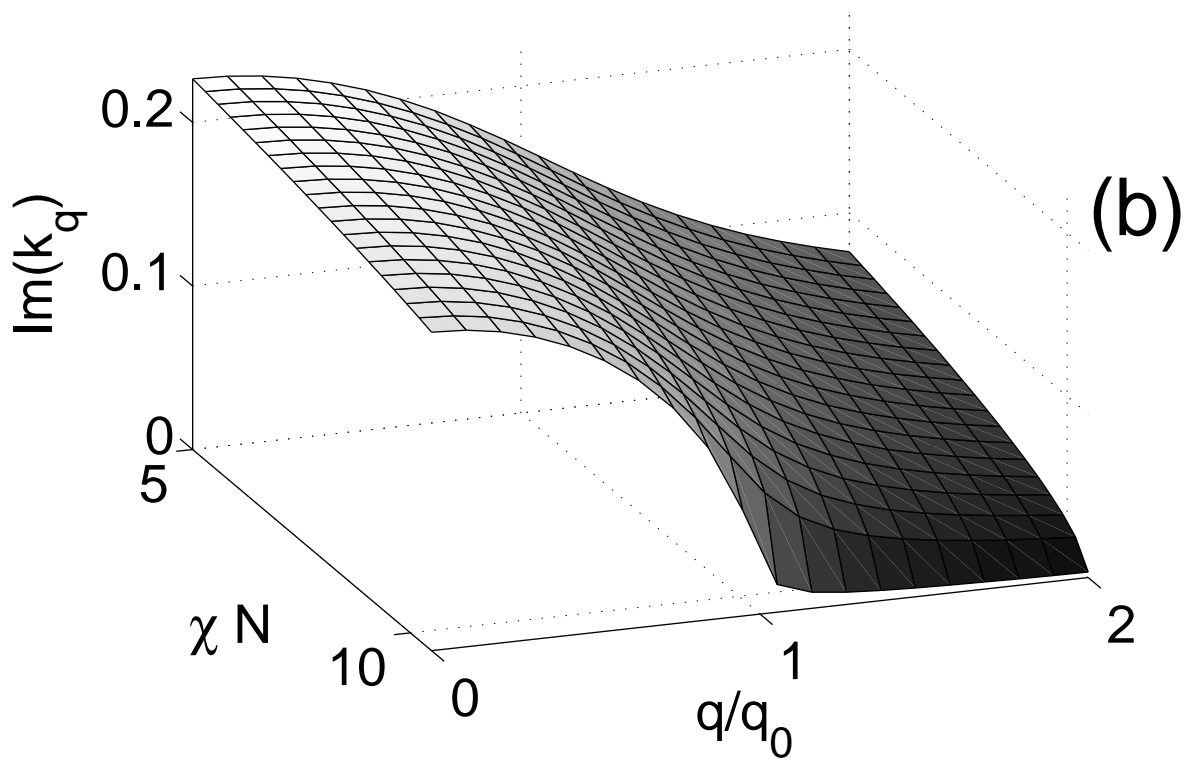
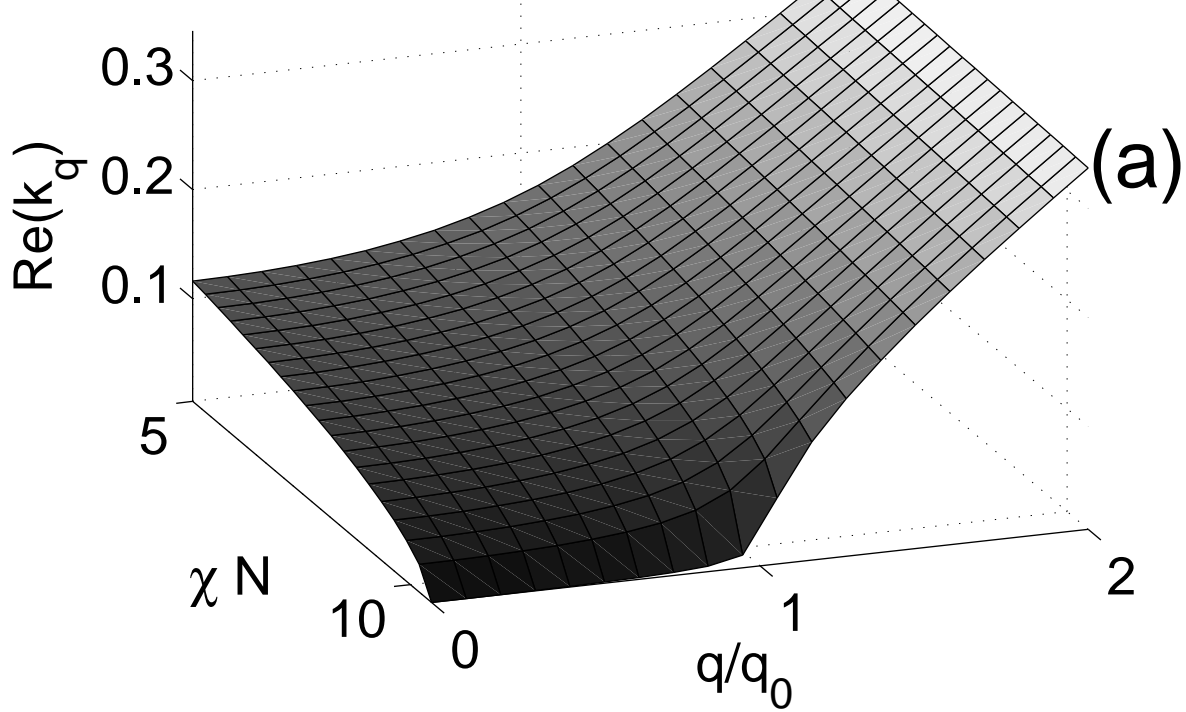


Fig. 1

Yoav Tsori + David Andelman

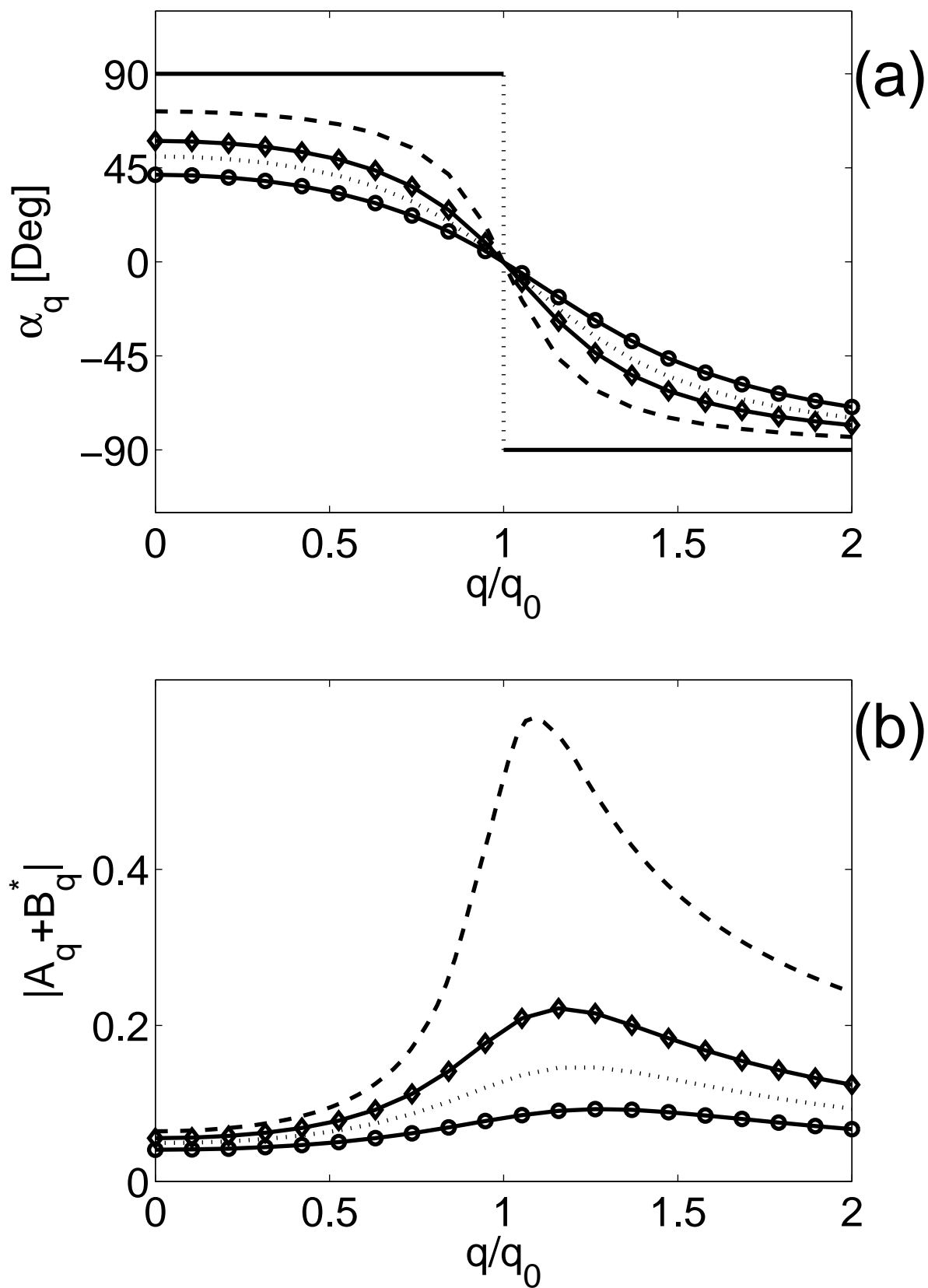


Fig. 2

Yoav Tsori + David Andelman

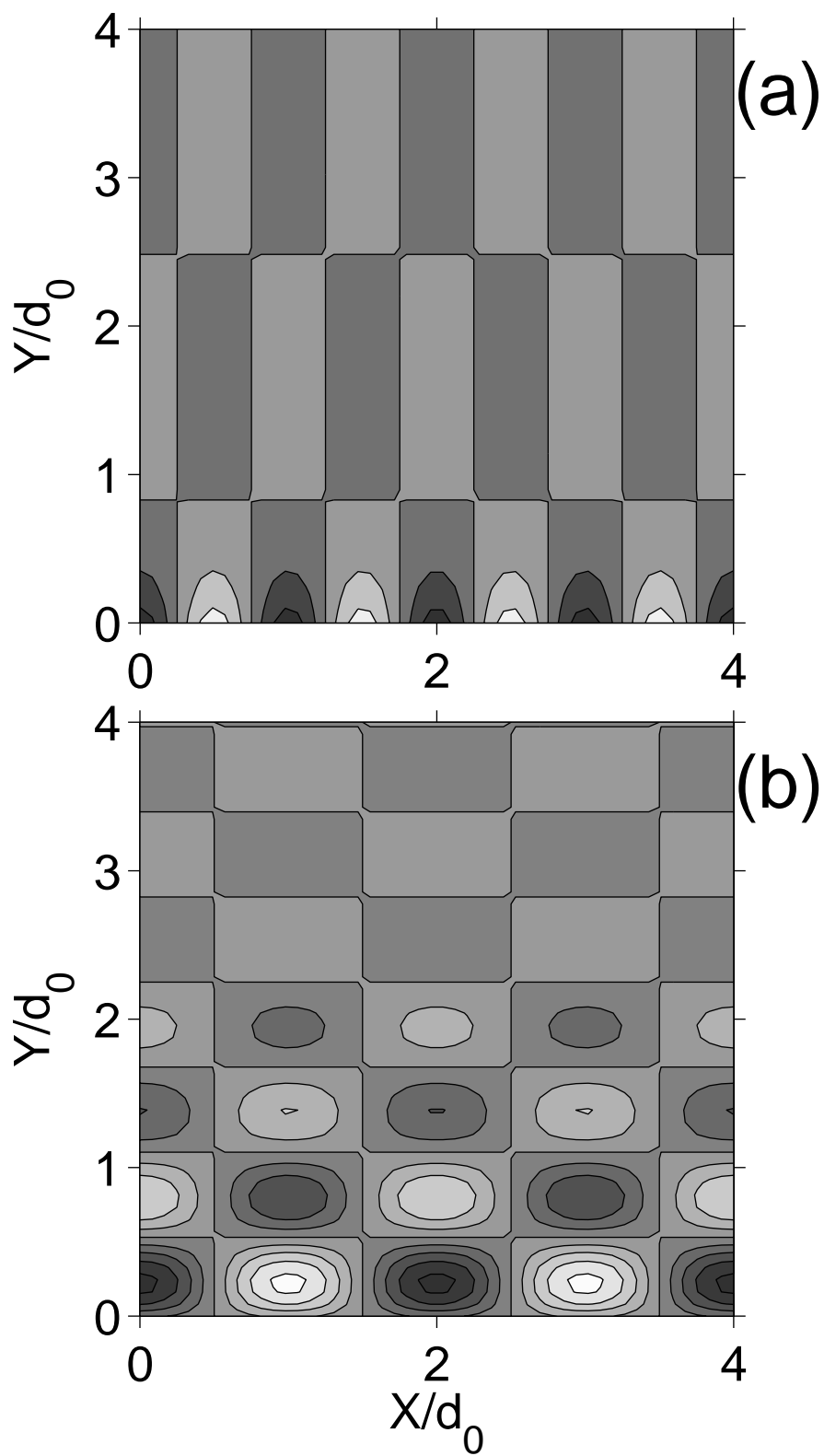


Fig. 3

Yoav Tsori + David Andelman

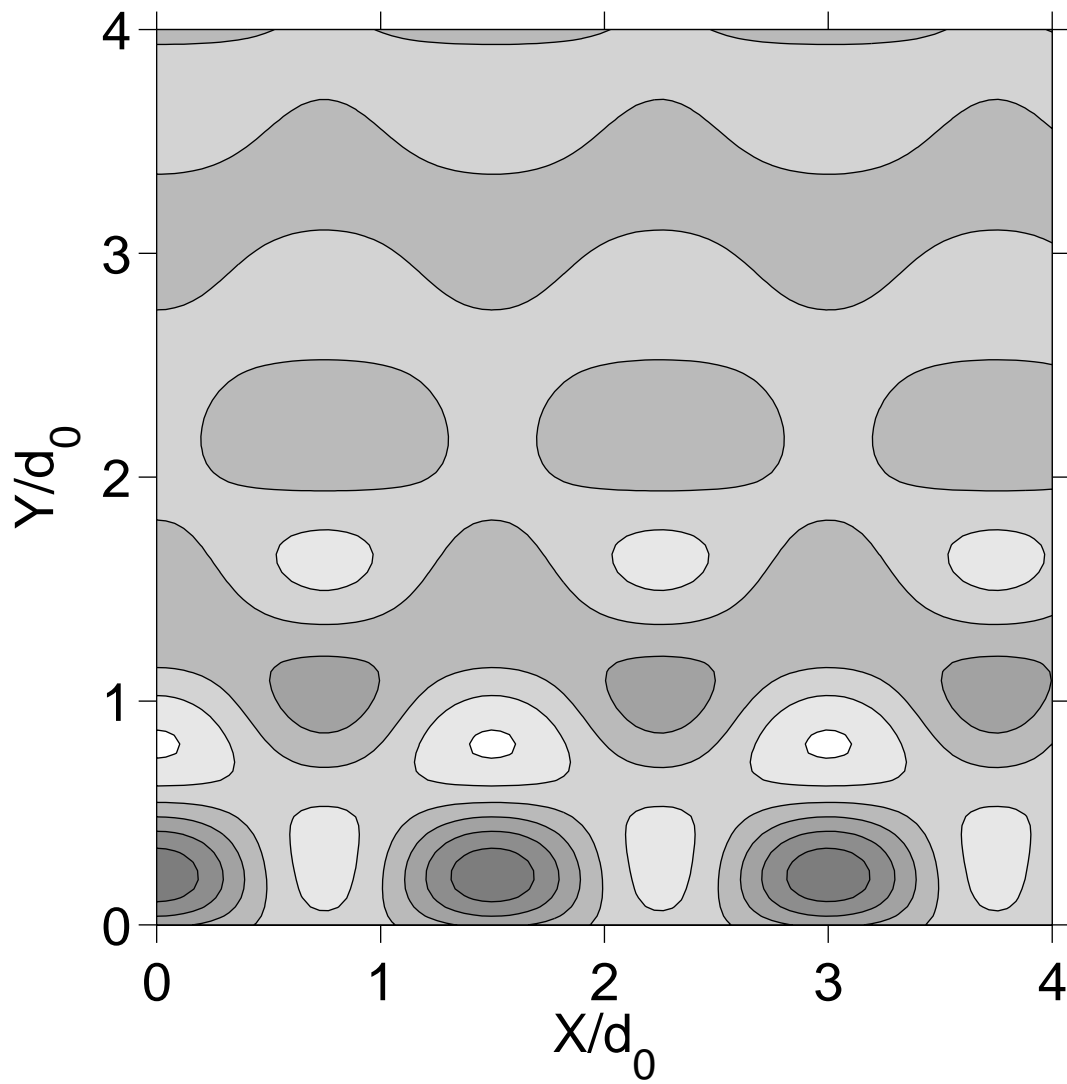


Fig. 4  
Yoav Tsori + David Andelman

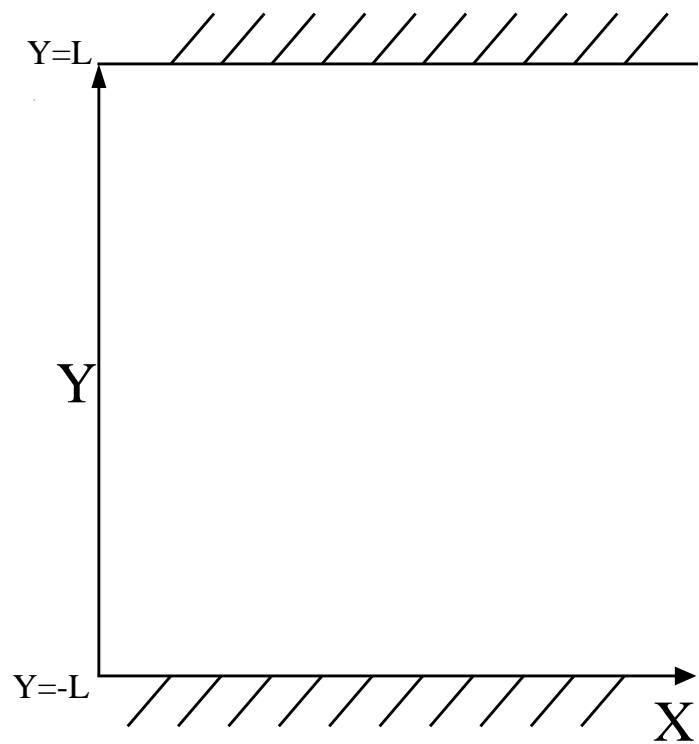


Fig. 5  
Yoav Tsori + David Andelman

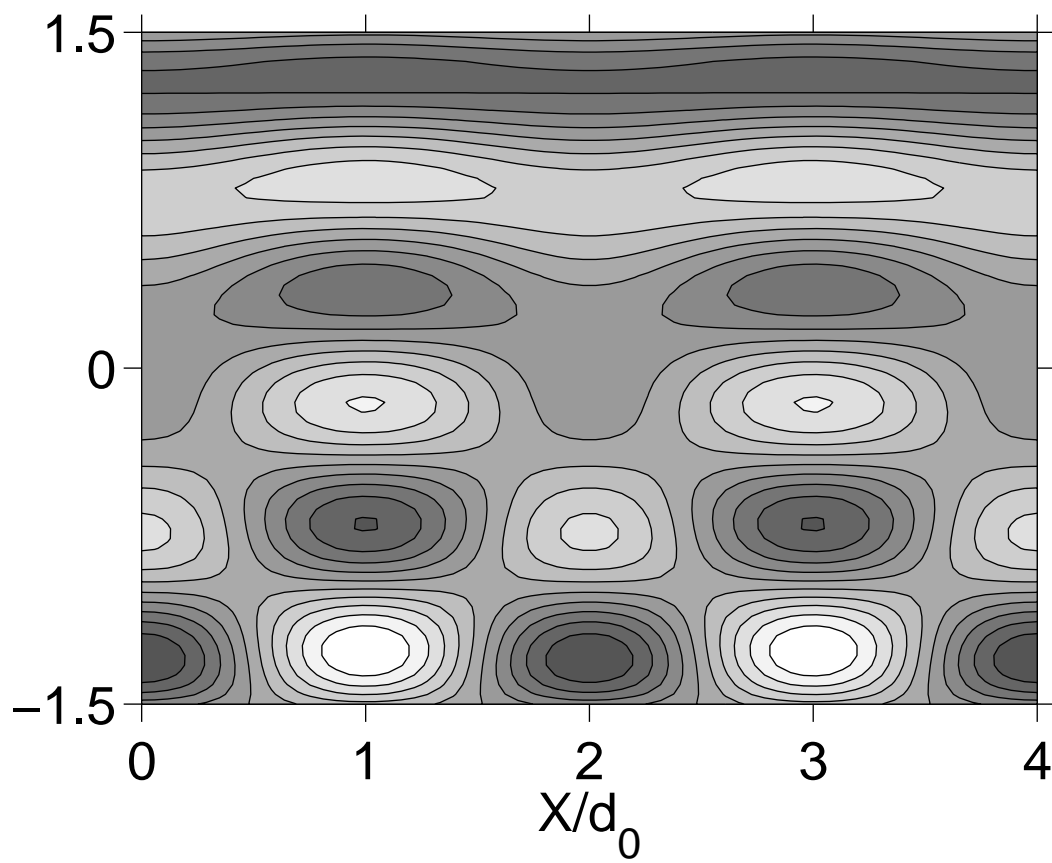


Fig. 6  
Yoav Tsori + David Andelman

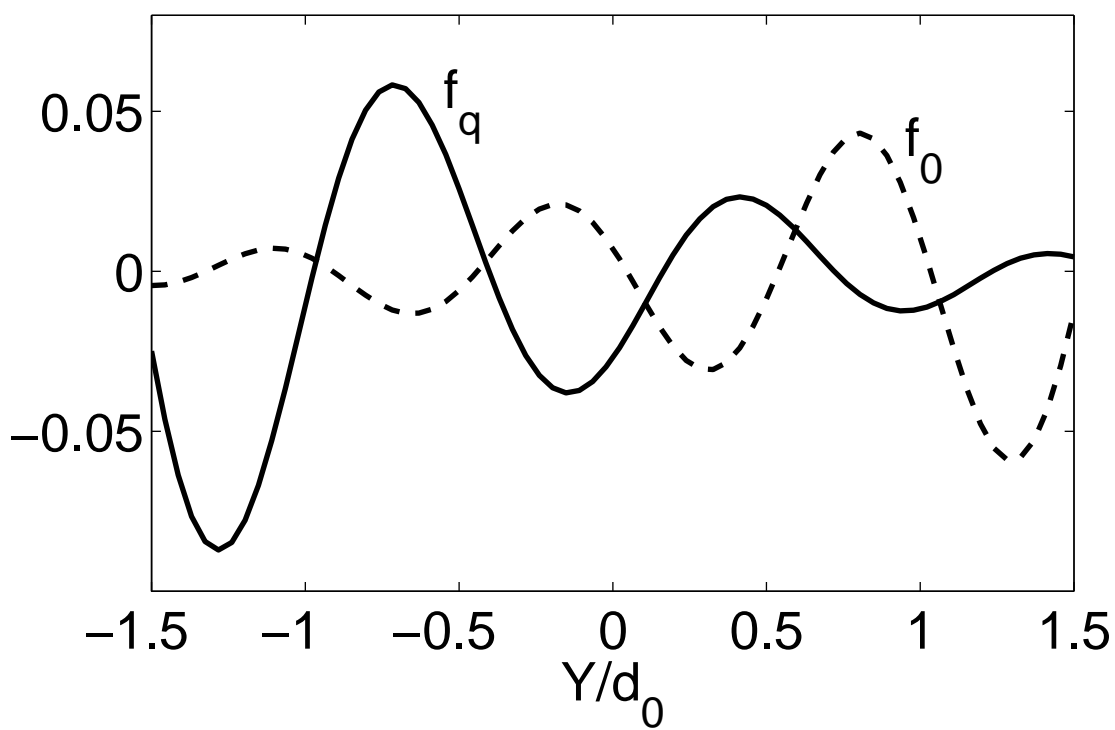


Fig. 7  
Yoav Tsori + David Andelman



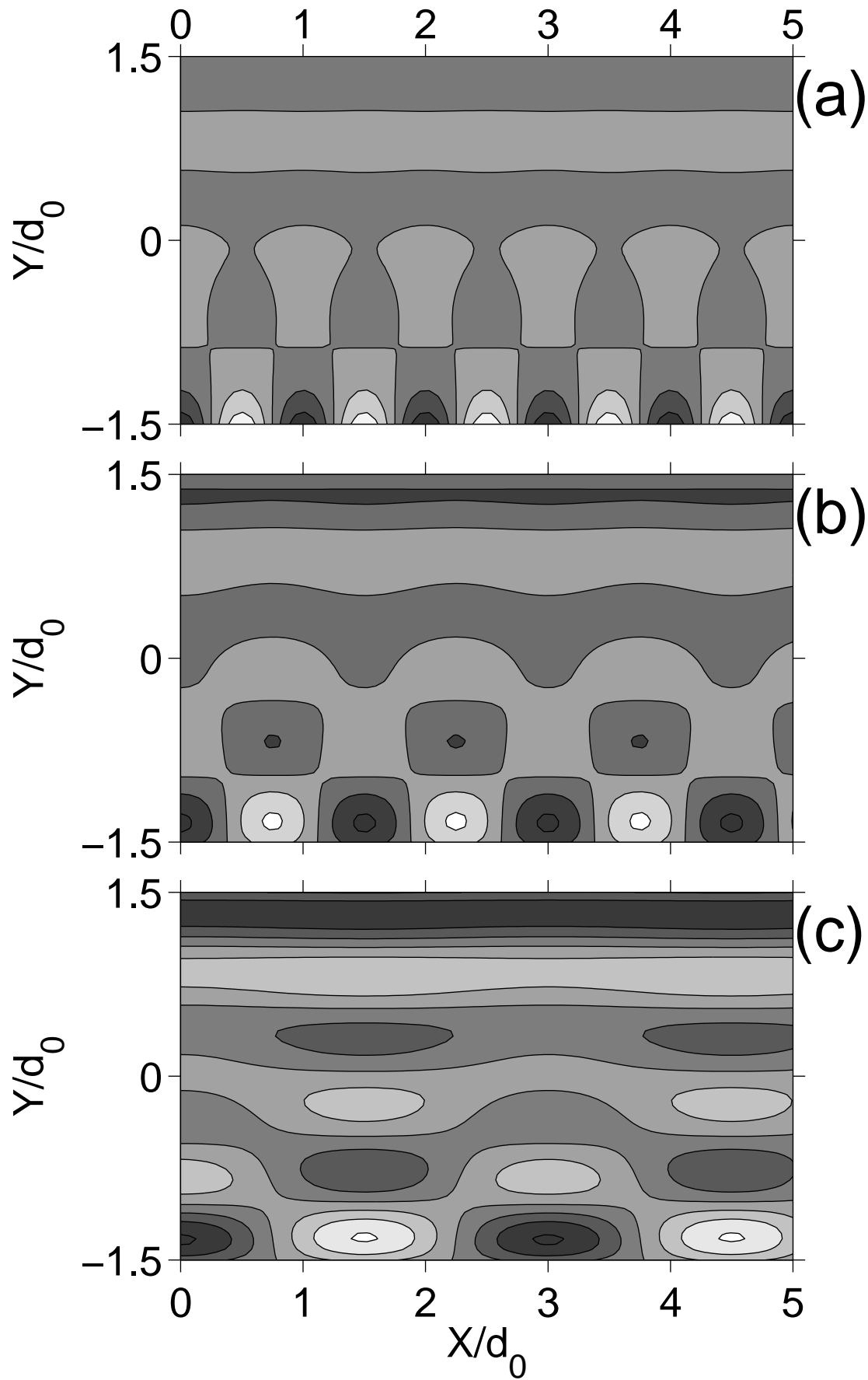


Fig. 8

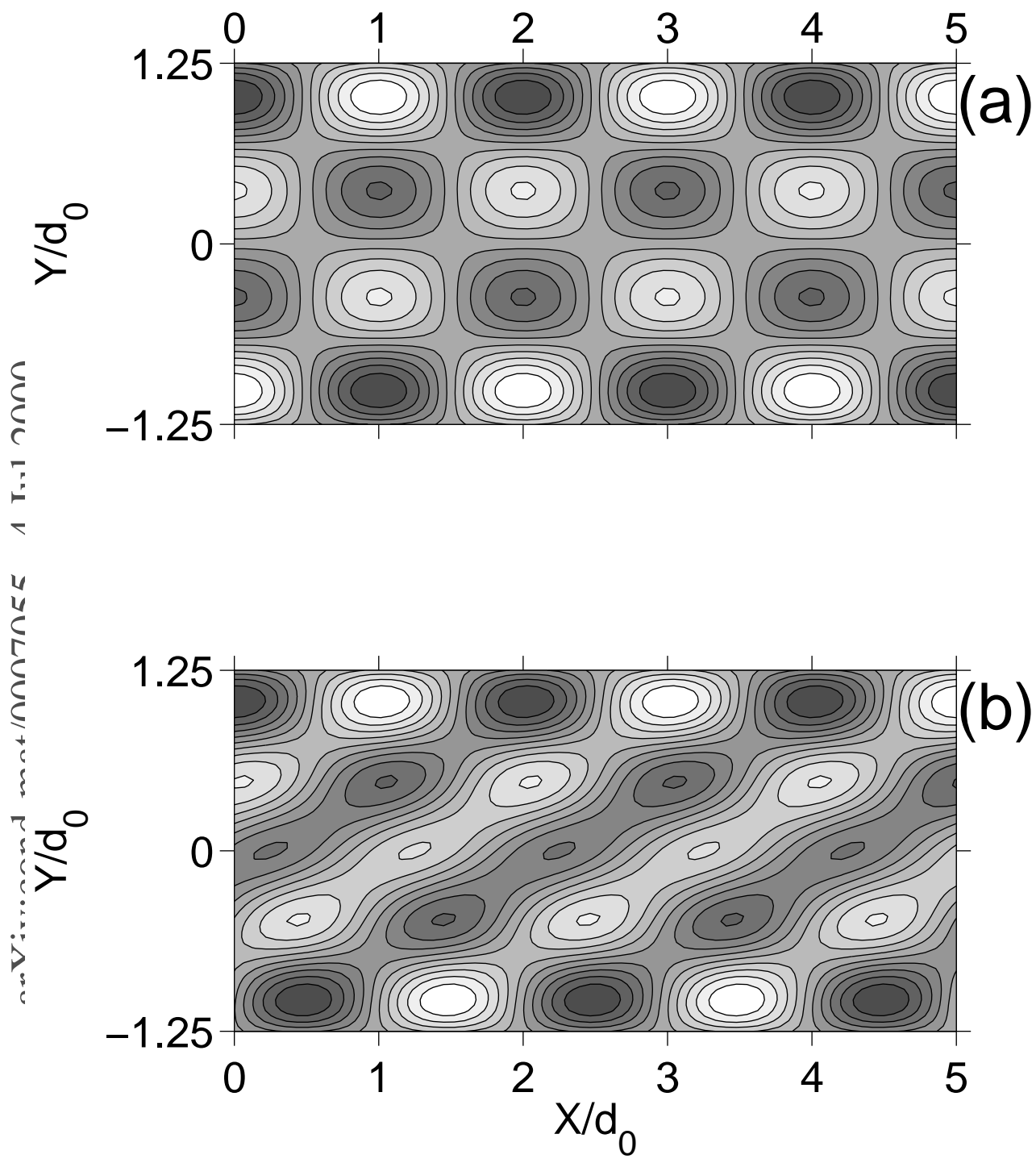


Fig. 9

Yoav Tsori + David Andelman

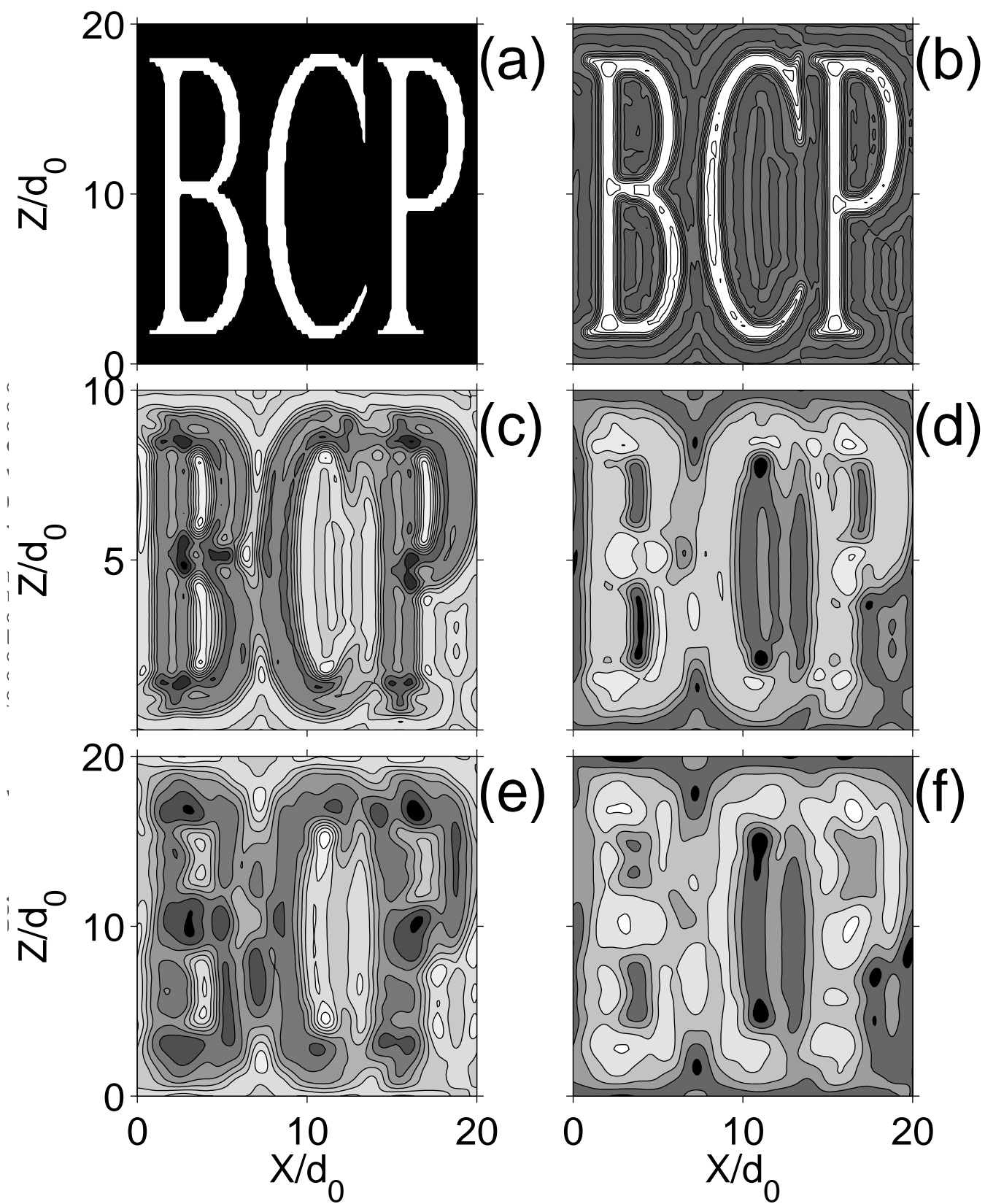


Fig. 10

Yoav Tsori + David Andelman

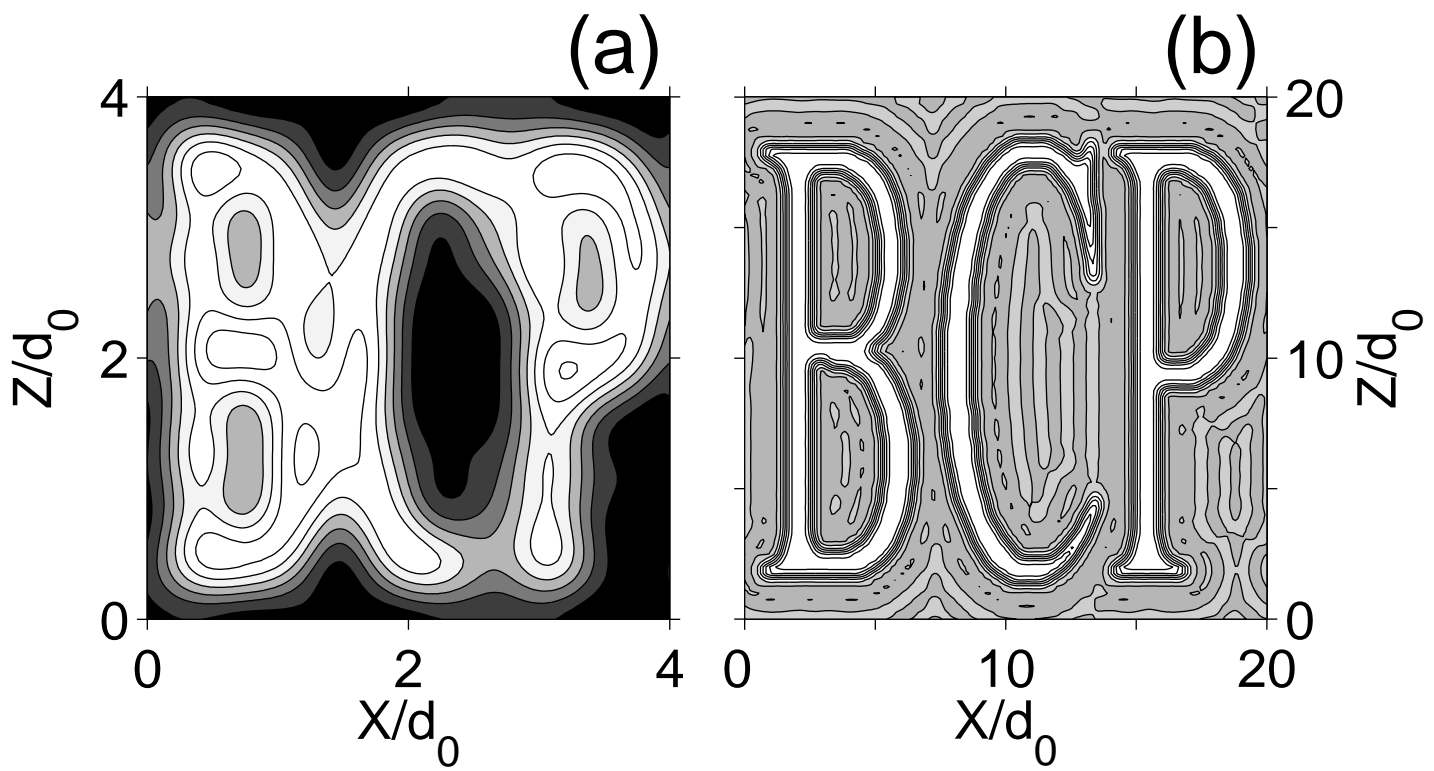


Fig. 11

Yoav Tsori + David Andelman

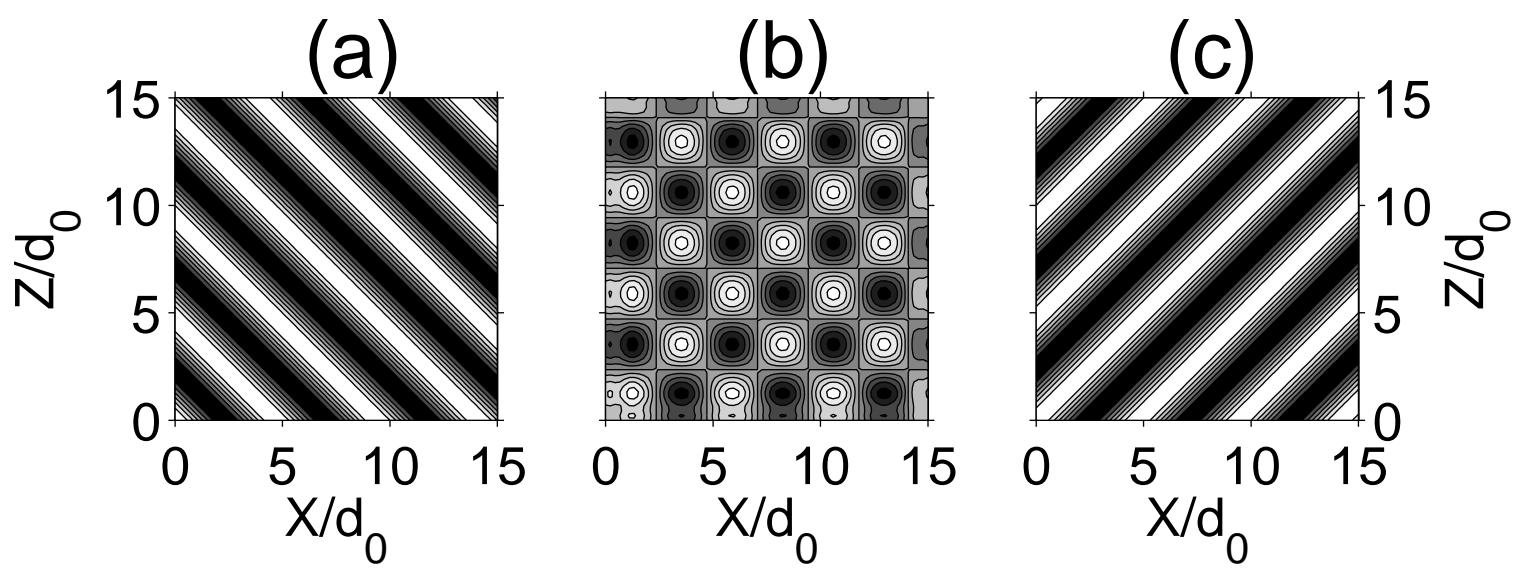


Fig. 12  
Yoav Tsori + David Andelman

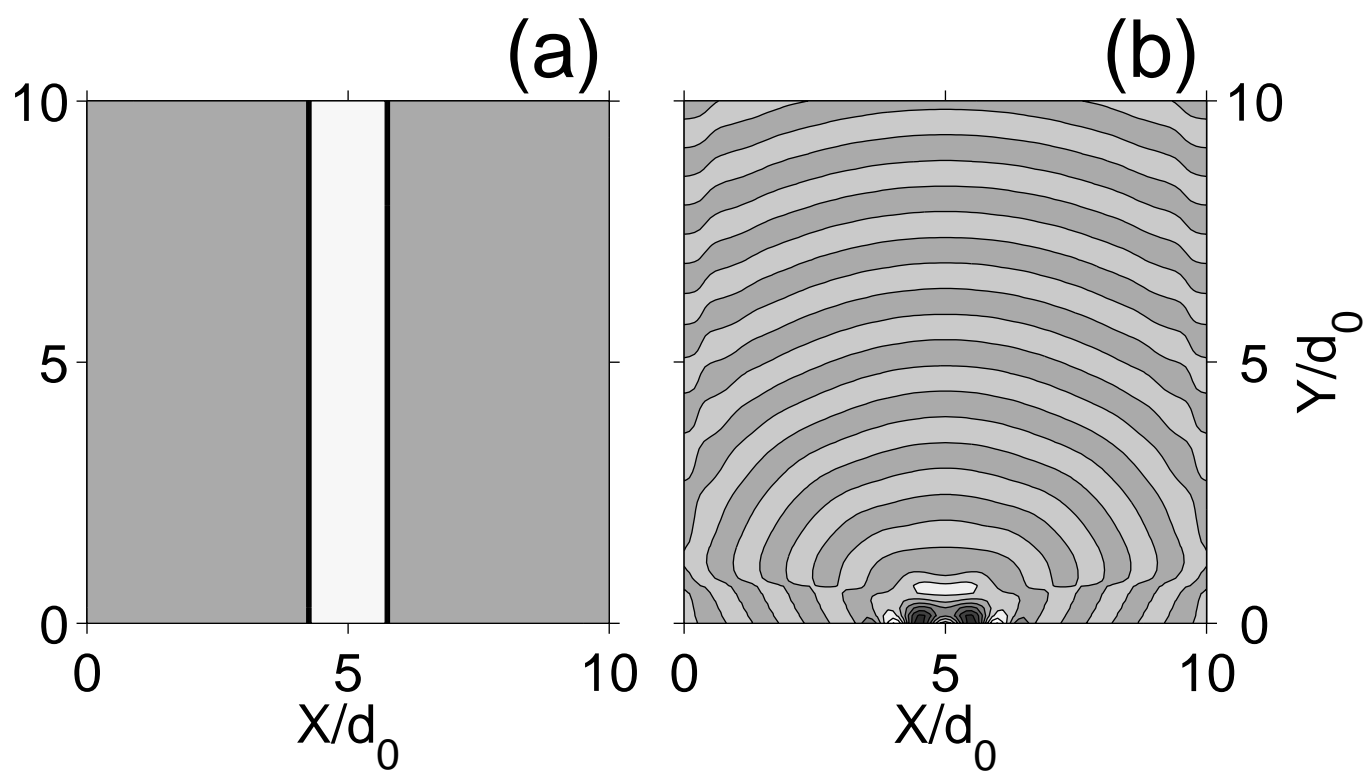


Fig. 13

Yoav Tsori + David Andelman

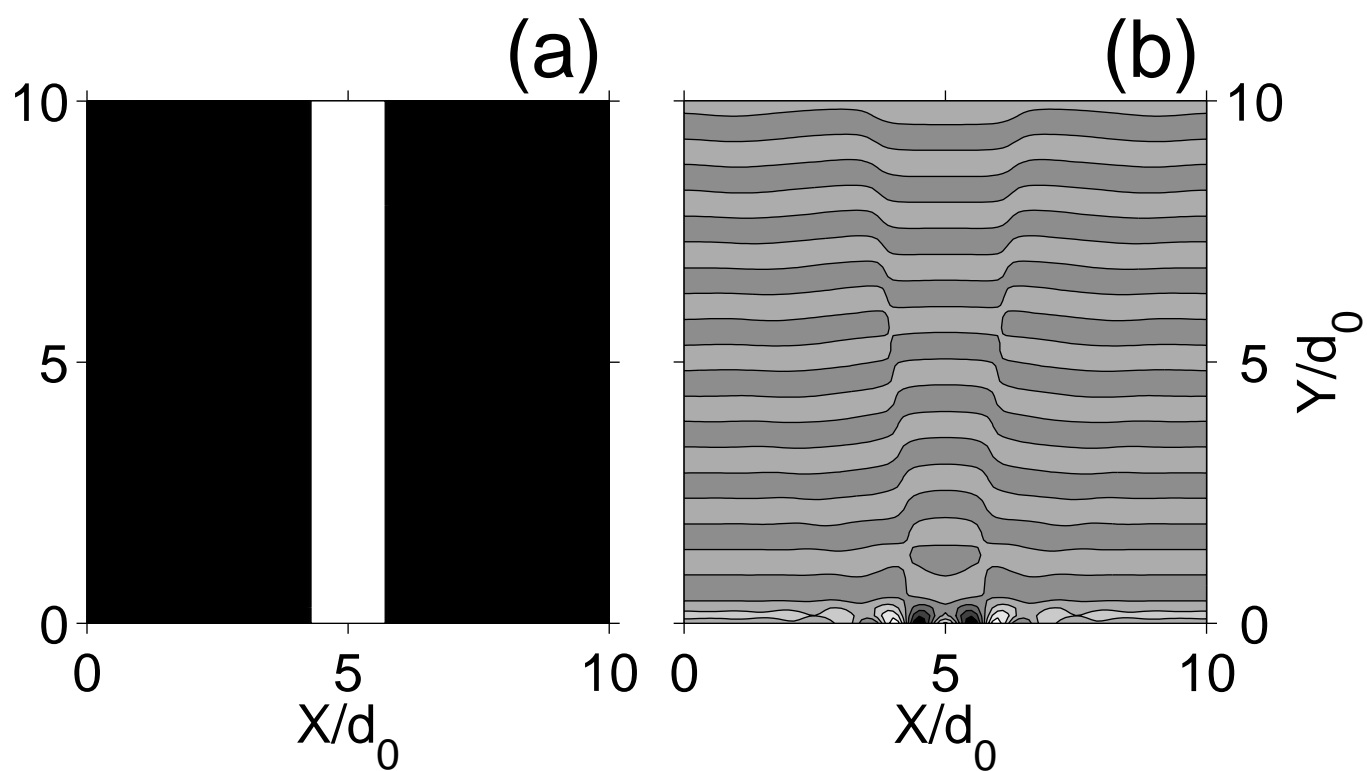


Fig. 14

Yoav Tsori + David Andelman